MSc thesis in Sustainable Energy Technology

Grid Impact Assessment of Unbalanced Penetration of Distributed Generation, Electrified Mobility & Heating in the Near and Far Future

Yme U. Wesseling

Aug 2023

A thesis submitted to the Delft University of Technology in partial fulfillment of the requirements for the degree of Master of Science in Sustainable Energy Technology

Abstract

The EU strives to lower greenhouse gas emissions. To reach this goal, many energy intensive processes in the residential sector such as heating and transportation will be electrified using heat pumps and electric vehicles (EVs) respectively. Simultaneously, a transition of electricity generation to sustainable sources will take place, necessitating an increased adoption of rooftop photovoltaic (PV) systems.

The adoption of PV systems, heat pumps and EVs, also known as low carbon technologies (LCTs), can increase three-phase unbalance in low voltage (LV) distribution networks as many of these components will be connected to a single phase of the three-phase network. Three-phase unbalance is undesirable in a three-phase system, as it causes among others, energy losses and a suboptimal use of network capacity.

The aim of this thesis is to evaluate the impact of different combinations and penetration levels of LCTs on three-phase unbalance in different real LV distribution networks through simulations and how unbalance is affected by LCT location, season and LCT control schemes.

Simulations were performed on six different grids, varying in level of urbanization and loading, with increasing levels of LCT penetration (0%, 50%, 80%, 100%). In these simulations, LCTs were integrated in varying combinations (PV & EV, PV & HP and PV & EV & HP). For every simulation, the maximum and mean voltage unbalance factor (VUF) was determined. Seasonal effects and the effect of an LCT control scheme were also evaluated.

Simulations showed that the voltage unbalance factor exceeded the legal limit of 3% for two of the six grids for high levels of LCT penetration when all LCTs are integrated. Combining all three LCTs resulted in the highest unbalance levels. Varying the locations of the LCTs resulted in significant differences in unbalance levels. Comparing a winter week with a summer week, the overall unbalance is similar, however, the contribution of the PV systems to the unbalance is increased, while the contribution of EV chargers and heat pumps is decreased. The effect of the LCT control scheme was limited.

As the integration of LCTs will increase considerably in the near future, three-phase unbalance levels exceeding the limit of 3% will occur more often. To prevent unbalance levels from structurally exceeding the legal limit of 3%, more effective control schemes should be designed and implemented.

Contents

List of Figures

List of Tables

Acronyms

LCT low carbon technology v
EV electric vehicle v
PV photovoltaic v
DSO distribution grid operator 1
LV low voltage v
MV medium voltage
HP heat pump 36
SOC state of charge 18
VUF voltage unbalance factor v
ACM Autoriteit Consument & Markt 26

1 Introduction

1.1 Background

The European Green Deal established the aim of net zero greenhouse gases emission in the EU by 2050 [1]. To reach this goal, many energy intensive processes will be electrified in the near future, in combination with a transition of electricity generation to sustainable sources. Low carbon technologies (LCTs) such as heat pumps, electric vehicles (EVs) and rooftop photovoltaic (PV) systems are projected be increasingly integrated into the residential sector [2, 3, 4], in part due to various policies regulating emissions and promoting more sustainable technologies [5, 6].

However, this electrification of residential loads will increase the strain on the Dutch electrical grid, which is already nearing energy transport capacity limits in most of the country [7]. Apart from contributing to capacity issues, the adoption of LCTs can increase three-phase unbalance as many of these components will be connected to a single phase of the three-phase distribution network. Three-phase unbalance is undesirable in a three-phase system such as the Dutch electrical grid, as it causes among others, energy losses and a suboptimal use of network capacity [8].

It is important for distribution grid operators (DSOs) and policy makers to have an idea of three-phase unbalance levels in the future and the factors that influence it. As such, the evaluation of the three-phase unbalance impact of LCTs is an active topic of research. In literature, while various simulation studies have been performed on separate LCTs types, few studies investigating the combined impact and different penetration levels of PV systems, EV chargers and heat pumps on three-phase unbalance have been performed. These studies are limited to relatively simple, single grids with a limited number of loads, and do not consider the effects of LCT locations and seasonal effects.

1.2 Research Aim

The aim of this thesis is to evaluate the impact of different combinations and penetration levels of LCTs on three-phase unbalance in different real LV distribution networks through simulations and how unbalance is affected by LCT location, season and LCT control schemes.

1.3 Thesis Structure

This thesis is structured as follows: first, in Chapter 2, the concept of three-phase unbalance and its causes and consequences are explained. Then, a study of the existing literature on the unbalance impact of LCTs is provided in Chapter 3. Next, in Chapter 4, the methodology

is presented. The results of simulations of various scenarios are shown and explained in Chapters 5, 6, 7 and 8, followed by the conclusion in Chapter 9.

2 Three-Phase Unbalance

This chapter aims to introduce the concept of three-phase unbalance. Section 2.1 explains the use of three-phase systems in the Netherlands. Next, Sections 2.2 and 2.3 present causes and consequences of three-phase unbalance. Finally, various metrics used to quantify three-phase unbalance are presented in Section 2.4.

2.1 Three-Phase system

The electricity grid in the Netherlands delivers electrical power through a three-phase network. In this network, the electrical power is generated in the form of three simultaneously generated alternating voltages that are shifted in phase with respect to each other, as can be seen in Figure 2.1. Most houses constructed before 2010 are connected to only one of the phases of the network. Houses built since 2010, public and commercial buildings have a three-phase connection. The performance of the three-phase system is optimal when the phases are balanced. However, due to several causes three-phase unbalance can occur resulting in a difference in voltage, current or phase angle from the balanced conditions [9].

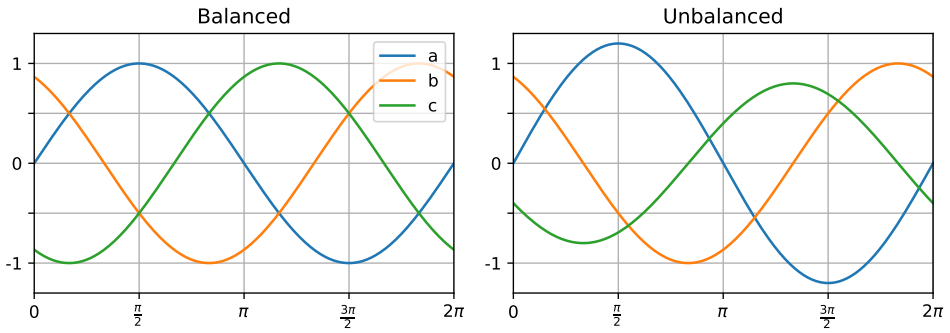

Figure 2.1: An example of balanced and unbalanced three-phase voltages

2.2 Causes of three-phase unbalance

Three-phase unbalance can be caused by several reasons. First, single-phase customers are often unevenly distributed over the three phases. Second, customers have a random and different load behaviour. Third, the network structure can be asymmetrical over the three phased, fourth there can be unbalanced faults in the network, and fifth uneven generation of energy [8]. This thesis focuses on the first two causes.

2.2.1 Uneven Loading

The effect of the uneven distribution of single-phase customers over the three phases and the random and different load behaviour of customers is the same: single-phase loads being unevenly distributed over the three phases causing structural three-phase unbalance. The increasing integration of large single-phase loads such as heat pumps and EV chargers [10] will lead to an increase in three-phase unbalance. Even though the new installations may be equally distributed over the three phases, the stochastic nature of the demand due to customer behaviour will introduce uneven loading over the different phases. PV systems do not have an unequivocally negative effect on the three-phase unbalance [**?**].

2.2.2 Structural Asymmetries

Structural asymmetries in distribution networks can cause three-phase unbalance similarly to uneven loading. However, in this case it is not the uneven load impedances causing the unbalance but the uneven self and mutual impedances in the lines [8]. The distribution networks used in this thesis do not contain single-phase feeders, as a result no structural asymmetry is expected.

2.2.3 Unbalanced Faults

Faults are unbalanced when they do not affect the three phases equally, resulting in three-phase unbalance. The following types of faults can cause unbalance [11].

- Line-to-line short circuit
- Line-to-ground short circuit
- Double line-to-ground short circuit
- Line-to-line-to-ground short circuit
- Single-phase broken-line fault
- Double broken-line fault

2.3 Consequences

Three-phase unbalance is generally undesirable as the voltages or currents are not equally distributed over the phases, leading to a higher peak voltage or current than necessary. In case of long-term three-phase unbalance, network capacity must be increased to account for the higher peak values. Additionally, the capacity of the phase(s) carrying less current is not fully utilized. The costs of this asset reinforcement are considerable, as quantified in [12].

Another consequence of three-phase unbalance, is increased power losses. Higher peak currents lead to higher thermal losses in power cables. Power losses also occur due to the fact that the neutral wire, which in balanced conditions carries no power, carries power which is not used [8].

2.4 Three-phase Unbalance Metrics

There are various metrics to quantify the magnitude of three-phase unbalance in voltage or current. The choice of metric is based on the measured variables and for comparison purposed on the metrics used in related research. The following metrics use a variety of measured quantities in a three-phase system. An overview of all metrics, and the quantities used, is given in Table 2.1. The definitions of all metrics will be given in the next paragraphs.

2.4.1 Voltage Unbalance Metrics

Voltage unbalance metrics are used to quantify three-phase unbalance when measuring voltage levels. We use the following quantities:

V_a, V_b, V_c:	Phase voltage for phase a, b or c
V_{ab}, V_{bc}, V_{ca}:	Line-to-line voltages
V_p, V_n:	Positive and negative sequence voltage components

IEEE Definition 1

The IEEE standard test procedure for polyphase induction motors and generators defines voltage unbalance as the ratio between the maximum phase voltage deviation from the average phase voltage and the average phase voltage as shown in Equation 2.1 [13].

$$\text{unbalance} = \frac{\max\{|V_a - V_{\text{avg}}|, |V_b - V_{\text{avg}}|, |V_c - V_{\text{avg}}|\}}{V_{\text{avg}}} \tag{2.1}$$

Where:

$$V_{\text{avg}} = \frac{V_a + V_b + V_c}{3}$$

Line Voltage Unbalance Rate (NEMA Definition)

Where the IEEE definition 1 uses the phase voltages, NEMA defines the voltage unbalance as the ratio between the maximum line voltage deviation from the average line voltage and the average line voltage as shown in Equation 2.2 [14].

$$\text{LVUR} = \frac{\max\{|V_{ab} - V_{\text{avg}}|, |V_{bc} - V_{\text{avg}}|, |V_{ca} - V_{\text{avg}}|\}}{V_{\text{avg}}} \tag{2.2}$$

Where:

$$V_{\text{avg}} = \frac{V_{ab} + V_{bc} + V_{ca}}{3}$$

Unbalance Factor (CIGRE Definition)

CIGRE recommends using the definition shown in Equation 2.3 [14].

$$\text{Unbalance Factor} = \sqrt{\frac{1-\sqrt{3-6\beta}}{1+\sqrt{3-6\beta}}} \tag{2.3}$$

where β is defined as:

$$\beta = \frac{|V_{ab}|^4 + |V_{bc}|^4 + |V_{ca}|^4}{(|V_{ab}|^2 + |V_{bc}|^2 + |V_{ca}|^2)^2} \tag{2.4}$$

Voltage Unbalance Factor

Pillay et al. [15] describes the *"True Definition"* of voltage unbalance as the ratio between the negative sequence voltage component and the positive sequence voltage component, as shown in Equation 2.5. This definition takes into account both the voltage magnitudes as well as the voltage angles.

$$\%\text{VUF} = \frac{\text{negative sequence voltage component}}{\text{positive sequence voltage component}} \cdot 100 \tag{2.5}$$

$$V_n = \frac{V_{ab} + \alpha^2 \cdot V_{bc} + \alpha \cdot V_{ca}}{3} \tag{2.6}$$

$$V_p = \frac{V_{ab} + \alpha \cdot V_{bc} + \alpha^2 \cdot V_{ca}}{3} \tag{2.7}$$

where $\alpha = 1\underline{/120^\circ}$

2.4.2 Current Unbalance Metrics

Like voltage unbalance, current unbalance occurs when the line currents differ from one another, or when the phase difference of the line currents is not 120°. Current unbalance can be measured in many different ways. The choice of metric will depend on available measurements.

Current Unbalance Factor

The current unbalance factor (CUF) is the current equivalent of the voltage unbalance factor. It is defined as the ratio between the negative sequence current and the positive sequence current as shown in Equation 2.8 [16]. The CUF is the most often used current unbalance metric [17].

$$\text{CUF} = \frac{I_n}{I_p} \tag{2.8}$$

$$I_n = \frac{I_a + \alpha^2 I_b + \alpha I_c}{3} \tag{2.9}$$

$$I_p = \frac{I_a + \alpha I_b + \alpha^2 I_c}{3} \tag{2.10}$$

Complex Current Unbalance Factor

The current unbalance factor can be expanded to the complex current unbalance factor (CCUF) as shown in Equation 2.11 [18]. This metric takes into account the phase angle of the line currents as well as opposed to the CUF, which only uses the magnitudes of the line currents.

$$\overline{\text{CCUF}} = \frac{\overline{I_a} + \alpha^2 \overline{I_b} + \alpha \overline{I_c}}{\overline{I_a} + \alpha \overline{I_b} + \alpha^2 \overline{I_c}} \tag{2.11}$$

Current Unbalance Indicator

The current unbalance indicator (IUNB) is defined as shown in Equation 2.12 [19].

$$\text{IUNB} = \frac{\sqrt{I_{eq}^2 - I_p^2}}{I_{eq}} \tag{2.12}$$

$$I_{eq} = \sqrt{\frac{I_a^2 + I_b^2 + I_c^2 + I_n^2}{3}} \tag{2.13}$$

Unbalance Indicator

The unbalance indicator is a simple indicator defined as the ratio between the largest deviation from the average rms current and the mean rms current as shown in Equation 2.14 [20].

$$U_i = \max\{|I_{\text{avg}} - I_{\text{min}}|, |I_{\text{max}} - I_{\text{avg}}|\} / I_{\text{avg}} \tag{2.14}$$

Current Unbalance Index

The current unbalance index (CUI) is another simple metric defined as the Euclidean sum of the squared current deviations compared to the equivalent current as shown in Equation 2.15.

$$\sqrt{\left(d_{I_a}^2 + d_{I_b}^2 + d_{I_c}^2\right)/3} \tag{2.15}$$

$$d_{I_i} = \frac{\sqrt{|I_i^2 - I_{eq}^2|}}{I_{eq}} \tag{2.16}$$

2.4.3 Phase Unbalance Metric

Adekitan has proposed a definition of phase unbalance that only takes into account the phase differences of the voltage or current waveforms [21].

$$\text{Ph UB} = \frac{\max\{|\angle ab - 0°|, |\angle bc - 240°|, |\angle ca - 120°|\}}{\angle 120°} \tag{2.17}$$

2.5 Overview of Metrics

Various factors influence the choice of unbalance metric, such as which variables are being measured. The phase voltage and current and the line-to-line voltages are relatively easy to measure, however, phase angles are not considered. In the VUF the phase angles are taken into account [15].The choice of metric also depends on the metric used in reference material for comparison purposes. An overview of which metrics use which measured variables is shown in Table 2.1.

Acronym	Name	V_{ph}	V_{LL}	V_p, V_n	I_{ph}	I_p, I_n	angle
IEEE 1		x					
LVUR			x				
CIGRE			x				
VUF				x			
CUF						x	
CCUF						x	
IUNB					x	x	
UI					x		
CUI					x		
PHUB							x

Table 2.1: Summary of unbalance metrics

For this research, the voltage unbalance factor was chosen as this is the most commonly used metric in literature as well as the metric used to define unbalance limits for Dutch DSOs [22].

3 Literature Review

This chapter presents a review of the current state of research on the three-phase unbalance impact of various LCTs. First, research on the individual impact of PV systems, EV chargers and heat pumps is discussed in Sections 3.1, 3.2 and 3.3 respectively. Next, research on the combined impact of LCTs is discussed in Section 3.4. Finally, the gap in research this thesis aims to fill is presented in Section 3.5

3.1 Impact of PV

There have been many studies performed on the impact of single- and three-phase PV systems on voltage unbalance in low voltage distribution networks. The impact on current unbalance is still a less explored subject.

3.1.1 Voltage Unbalance

Shahnia et al. and Ruiz-Rodriguez studied the impact of single-phase rooftop PV installations on LV distribution networks using probabilistic simulations [23, 24]. Both studies randomized the location and phase connection of the PV installations, as well as the rated power and penetration levels. The results of these studies were similar, increased penetration of small single-phase PV systems (5 kW) can have a stabilizing effect on voltage unbalance in the network. However, increased penetration of large single-phase PV systems (15 kW) increases voltage unbalance. Shahnia et al. were also able to conclude that PV installations further from the beginning of the LV feeder had a bigger impact on voltage unbalance than PV installations closer to the beginning of the feeder [23].

Gonzalez et al. and Mrehel et al. studied the impact of single-phase PV systems using simulations of set scenarios [25, 26]. These scenarios specified the amount and ratings of PV systems and to which building in the network and phase these systems were connected. Both authors considered worst case scenarios, having all PV systems connected the same phase in a feeder. Both studies found results similar to those of the previously mentioned studies. Increased penetration of single-phase PV systems may introduce or reduce voltage unbalance depending on the power output of the PV systems.

Aramizu et al. simulated a large three-phase PV system connected to the IEEE 13 bus test feeder [27]. It was found that a three-phase connected PV installation could decrease the voltage unbalance in the network.

Sexauer et al. performed load flow simulations of various scenarios ranging from 0% to 50% distributed generation penetration, for weak or strong system strengths [28]. A penetration level of 50% means that the installed capacity of distributed generation sources is equal to

50% of the peak load of the system. Sexauer defines a strong system as one that is appropriately sized for the peak load, whereas a weak system has reduced cable sizing to emulate the effects of lack of investment due to the added capacity of distributed generation [28]. It was found that three-phase connected distributed generation systems such as PV systems and wind turbines generally do not increase the probability of voltage unbalance. Only when the distributed generation systems are allowed to provide uncontrolled var support is there an increase in voltage unbalance.

3.1.2 Current Unbalance

Chicco et al. studied three-phase current unbalance due to a large PV field on top of a building in Torino (Italy) [17]. Various current unbalance metrics were applied to the measurements to study their performance in identifying current unbalance. It was found that there was no significant structural unbalance caused by the PV system. However, when partial shading was introduced to one of eight arrays in the system, significant current unbalance occurred. It was noted that the current unbalance metrics TPU_I and $ITUD$ performed the best in quantifying unbalance taking into account harmonic distortion.

3.2 Impact of EV Chargers

Very few works in the literature have yet investigated the impact of single-phase EV chargers on phase unbalance.

Putrus et al. investigated the impacts of EV deployment on distribution networks [29]. Both single-phase home chargers and car park chargers were taken into consideration. Three scenarios were studied for various levels of EV deployment, an uncontrolled scenario, a scenario with off-peak charging control and a scenario using 'smart' charging, where the charging schedules are phased to spread out the load. It was found that in the case of low EV deployment (10% of households) there was a larger variation in current unbalance due to the lack of diversity. On the other hand, the voltage unbalance remained low due to the lower total load. In the case of high EV deployment (90% of households) it was found that the average current unbalance was lower, while the voltage unbalance increased due to the higher total load.

Ul-Haq et al. studied the impact of uneven EV charging in a LV distribution network in both an uncontrolled and a tariff based controlled case [30]. It was found that for an EV penetration level of 50% the voltage unbalance exceeds the allowed limit in the uncontrolled case. When tariff based control was introduced, the voltage unbalance did not exceed the limits.

Mejdi et al. analyzed the impact of a workplace parking lot with 54 EV chargers in Tunisia [31]. A simulation based on real user data showed that there was significant current unbalance introduced by the EV chargers. However, the voltage unbalance remained below the standard limit at all times.

3.3 Impact of Heat Pumps

Very little research has been performed on the phase unbalance impact of heat pumps exclusively. The research containing heat pump impact is often done in conjunction with PV and EV charger integration as discussed in the next section.

3.4 Combined Impact

There have been studies on the combined impact of PV, heat pump and EV charger integration on the voltage unbalance in a distribution network. The combined impact on current unbalance is however a largely unexplored area.

Al Essa et al. performed simulations of five scenarios on a single grid with a limited number of loads (<150) [32]. They used a base-case scenario with no PV, EV chargers or heat pumps, three scenarios with only PV, EV chargers and heat pumps at 100% penetration level and finally a scenario with 100% integration of PV single-phase PV systems, EV chargers and heat pumps [32]. The results showed that the distribution network could tolerate the integration of low-carbon technologies separately. However, the integration of EV chargers caused significant voltage unbalance, due to the large variability in demand compared to heat pumps.

Li et al. performed a Monte-Carlo simulation randomly assigning heat pumps and EV chargers at various penetration levels to households in a single network with a limited number of loads (<100) [33]. Similarly to Al Essa et al, Li et al. found that the integration of EV chargers has a significant effect on the voltage unbalance in the network, whereas the integration of heat pumps has a much smaller impact. In contrast to Al Essa et al., Li et al. performed a simulation using a control scheme based on time-of-use tariffs to lower the peak power consumption. It was shown that voltage violation periods were reduced relative to the uncontrolled case.

In both studies, seasonal effects and the effect of the locations of the LCTs are not investigated.

3.5 Research Gap & Contribution

Even though there has been extensive research on the impact of single-phase PV systems and EV chargers on three-phase unbalance in LV networks. The few studies on the combined impact of PV systems, EV chargers and heat pumps are performed on single grids with a limited number of loads without taking LCT locations and seasonal effects into account.

In this research, the impact of different combinations and penetration levels of LCTs on three-phase unbalance in different real LV distribution networks through simulations is evaluated, as well as how unbalance is affected by LCT location, season and LCT control schemes.

The parties that will benefit from the results of this research are DSOs, as they will gain insight in the impact of the coming electrification of central heating in homes and of electric private transport (EV) and of increased distributed generation will have on the unbalance of distribution grids.

4 Methodology

This chapter aims to present the models and how they are used in the simulations, as well as the experiments performed in this research. Section 4.1 presents the grids used in the simulations, followed by Section 4.2, which explains the models of the base load and LCTs. Next, in Section 4.3 it is explained how these models are connected to the grids. The distribution of the LCTs over the grids is explained in Section 4.4. Finally, the experiments are presented in Section 4.5.

4.1 Grids

Six LV distribution grids were provided by Enexis [34], a Dutch DSO as shown in Figures 4.1, 4.2 and 4.3. The grids were divided into lightly and heavily loaded variants where a lightly loaded grid is one where the DSO does not expect issues for increased LCT penetration and a heavily loaded grid is one where the DSO does expect issues. For each variant, lightly and heavily loaded, three levels of urbanization were provided: a rural, a suburban and an urban grid. Each grid consists of loads, corresponding to buildings, lines and fuses and one MV/LV transformer. The buildings are either commercial or residential, which has consequences for the amount and timing of the power consumption. All grids use a three-phase external grid component as the main power source. The grids will be expanded with LCTs such as PV systems, EV chargers and heat pumps depending on the number of buildings in the grid, to investigate the effect on the three-phase unbalance in the grid.

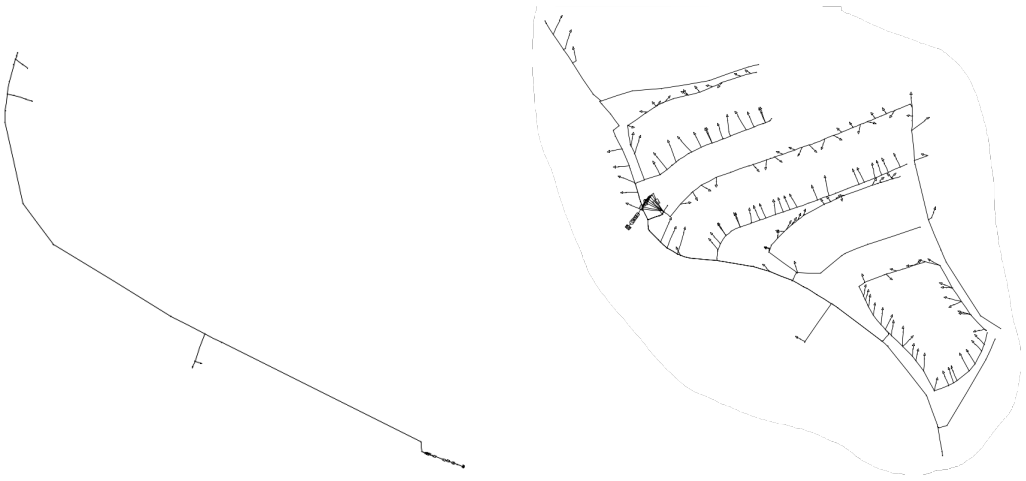

(a) Lightly loaded rural grid (b) Heavily loaded rural grid

Figure 4.1: The rural grids

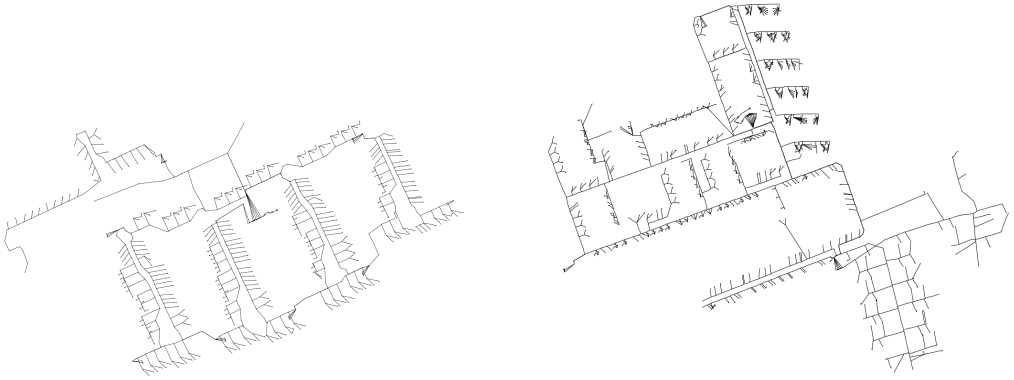

(a) Lightly loaded suburban grid (b) Heavily loaded suburban grid

Figure 4.2: The suburban grids

(a) Lightly loaded urban grid (b) Heavily loaded urban grid

Figure 4.3: The urban grids

Table 4.1 shows the amount of loads and nodes for each of the grids.

Grid	**Loads**	**Nodes**
Light Rural	3	28
Heavy Rural	138	546
Light Suburban	266	873
Heavy Suburban	480	1419
Light Urban	123	339
Heavy Urban	296	1512

Table 4.1: Characteristics of the six grids

4.2 Power Consumption Data and Models

The power consumption values of the load of the buildings (the base load) and LCTs, used in the simulations, are partially provided by Enexis (real-world data) and partially generated by models.

4.2.1 Base load

The base load of the grids consists of the total electrical load of residential and commercial buildings. Enexis has provided the yearly energy consumption of each building in the grid, as well as approximate power consumption profiles as published by the "Platform Verbruiksprofielen" [35]. Three variants of residential profiles and two variants of commercial profiles were used, shown in Figure 4.4. It can be seen that the commercial profiles have a higher peak during the day, while residential profiles have a peak in the evening.

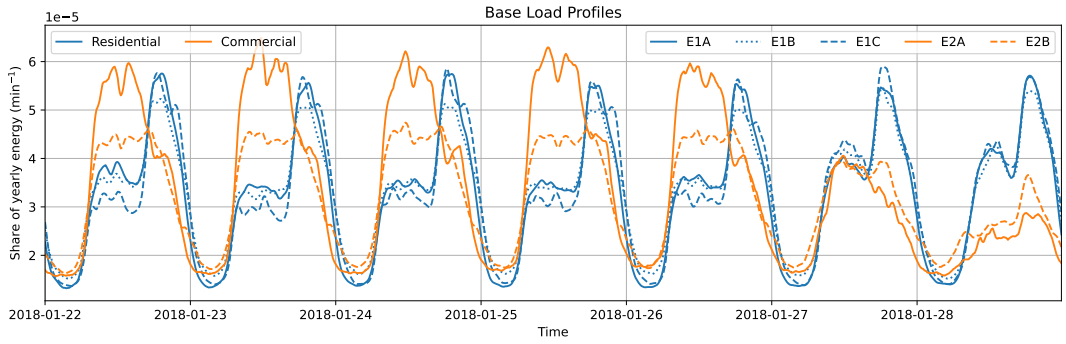

Figure 4.4: The 5 base profiles in the winter week used in the simulations.

where the different profiles are defined as follows:

- E1A: Residential profile without night meter
- E1B: Residential profile with night meter (from 23:00 to 7:00)
- E1C: Residential profile with night meter (from 21:00 to 7:00)
- E2A: Commercial profile without night meter
- E2B: Commercial profile with night meter

The approximate profiles were used to obtain the power consumption per 10-minute timestep as shown in Equation 4.1 where i represents a building.

$$P_i[t] = E_{i,\text{year}} * \text{profile}_i[t] \tag{4.1}$$

4.2.2 PV Systems

The PV systems used in the simulations were modelled after a real-world PV module, namely the HIT-N245 [36]. It is assumed that every PV system consists of 12 of these modules, resulting in a total rated power of 3 kW. In order to obtain realistic power generation values for the season and time of day, this model was fed the following weather data [37] from the region of the grids with a 1-minute timestep:

- Direct normal irradiance
- Diffuse horizontal irradiance
- Global horizontal irradiance
- Air temperature
- Wind speed

In order to ensure that not every PV system has the exact same power generation profile, the tilt angle and orientation of the PV modules were randomized (tilt angle: [10°, 50°], orientation: [0°, 360°⟩) resulting in 90 different PV systems. The output power of the PV module was calculated as follows [38]:

$$P = A_{\text{module}} * G_{\text{AOI}} * \eta_{\text{real}} * \eta_{\text{inv}} \tag{4.2}$$

Where:

A_{module}:	Surface area of the PV module
G_{AOI}:	Total incident irradiance on the PV module
η_{real}:	Efficiency of the PV module based on its temperature and the irradiation
η_{inv}:	Inverter efficiency, assumed to be 95%

Two weeks, one in the winter and one in the summer, of weather data were selected to obtain a total of 180 one-week PV profiles (90 for the winter week, 90 for the summer week). A summer and winter profile are shown in Figure 4.5, it can be seen that days are longer in the summer week, and more PV power is generated in the summer. Depending on the season used in the simulation, the 90 PV profiles were assigned randomly to the PV systems in the grids.

4.2.3 EV Chargers

The weekly profiles of the EV chargers were created using the following information:

- Arrival and departure time
- Arrival and departure state of charge (SOC)
- Rated charging current and battery capacity of various EVs [39]
- Constant current and constant voltage charging region models

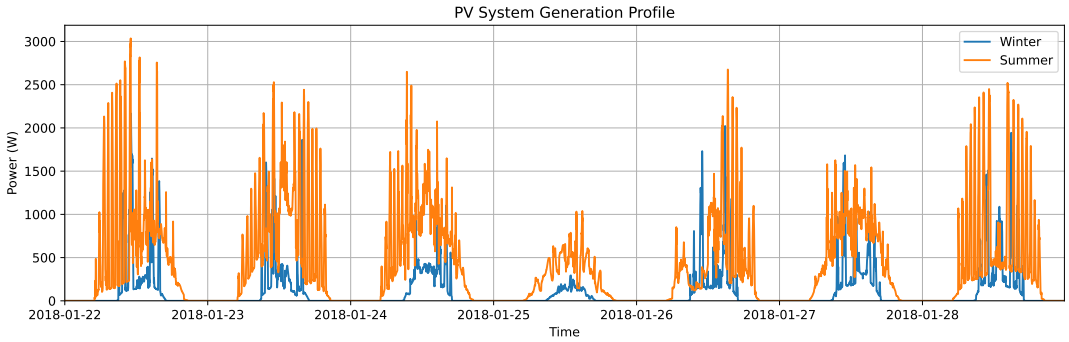

Figure 4.5: A winter and summer PV generation profile, the summer profile has been time-shifted to the winter week.

In order to include the constant current and constant voltage charging regions in the profiles, it was decided that charging below an SOC of 80% would be performed using the rated charging current. Charging at an SOC above 80% is performed using the constant voltage current if it is lower than the rated current. The calculation of the constant voltage current is shown in Equation 4.3.

$$I_{\text{cv}}(t) = 5 * (1 - \text{SOC}(t)) * I_{\text{rated}} \tag{4.3}$$

In total, 600 weekly profiles were created for the summer week, divided over three types of chargers: home, semi-public and public EV chargers. These charger types differ in parking time and frequency, a home charger has longer parking times than semi-public and public chargers but fewer charging events. For the winter week, the 600 profiles were changed to reflect a 30% increase in charging energy to account for increased energy used in heating the vehicle.

In the original model, vehicles had rated charging powers of either 11 kW, 16 kW or 22 kW. Since the upper limit of single-phase chargers is 7.4 kW due to the 35 A connection at 230 V, all vehicles could only be charged with three-phase chargers. To allow simulations with both single- and three-phase chargers, the rated charging power of EVs with a rated charging power of 11 kW was reduced to 7.4 kW. To increase the amount of single-phase chargers, 50% of EVs with a rated charging power of 16 kW were randomly selected. The charging power of these EVs was also reduced to 7.4 kW.

The first two days of the profiles of a home, semi-public and public EV charger are shown in Figure 4.6.

Averaged Charging

A simple charging control scheme was implemented in order to lower the peak power of the EV chargers. The charging power was averaged over the parking time of each vehicle as shown in Equation 4.4. This resulted in an additional 600 weekly EV charger power profiles.

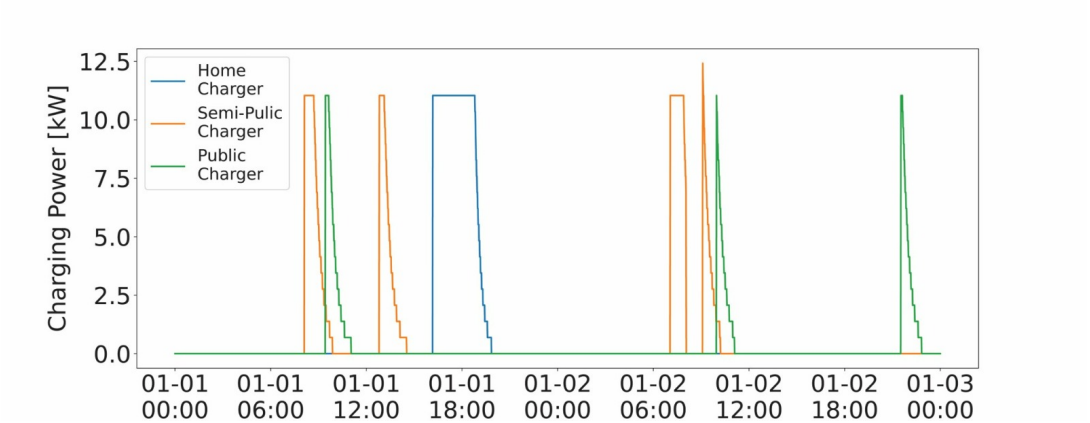

Figure 4.6: One of the EV charger power profiles

$$P_{\text{charging}}(t) = E_{\text{requested}} / t_{\text{parking}} \tag{4.4}$$

4.2.4 Heat Pumps

The model used to create the heat pump power profiles consisted two components, a building model and a heat pump model (Dimplex LIK 8MER) [40]. The building was modelled after a terraced house with brick walls, a wooden floor, clay roof tiles and insulation material. The heat conductivity value of the building was calculated using conductivity values of the materials used and the building dimensions.

The heat pump model contains two heating elements, a floor heating element to heat the building and a water tank heater to heat the domestic hot water. The domestic hot water heater is used twice a day, once at 06:00 and once at 19:00. The floor heating element was controlled based on the specifications of the building, desired temperature range, weather data, occupancy profile and heat pump specifications. 200 weekly power profiles were created for both the winter and summer weeks.

An example of a winter and summer heat pump profile is shown in Figure 4.7. The peaks are domestic water heating, while the other power consumption is the floor heating element.

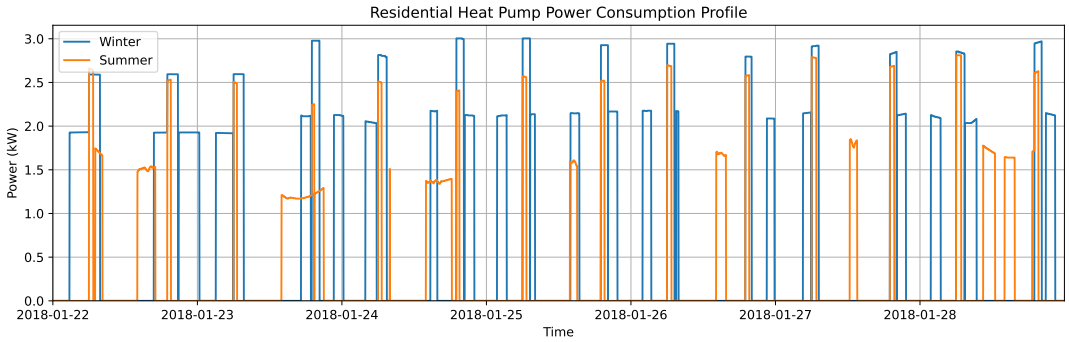

Figure 4.7: A winter and summer residential heat pump generation profile, the summer profile has been time-shifted to the winter week.

Low Power Mode

Again, a simple control scheme was implemented to reduce the peak power consumption of the heat pumps. The possible range of target temperatures was reduced from [21°C, 23°C] to [20°C, 21°C]. New winter profiles were created using the same model, but with these lower target temperatures, thus reducing the power needed to heat the building.

4.3 Phase Connections

In three-phase unbalanced simulations, the number of phases and the phase to which a component is connected are vital characteristics. Two types of phase connections were considered, three-phase wye connections and single-phase phase to neutral connections. Single-phase connections can be connected to any of the three phases.

4.3.1 Base Load

The phase connections of the base load components were provided by Enexis. These phase connections were used in the simulations.

4.3.2 Heat Pumps and PV Systems

Both heat pumps and PV systems are assumed to be single-phase components as both models have nominal power values below the legal limit for single-phase components [41]. When a heat pump or PV system was assigned to a single-phase connected building, the heat pump or PV system was connected to the same phase as the building. In the case of a three-phase connected building, the heat pump or PV system was connected to a single randomly chosen phase.

4.3.3 EV Chargers

The phase connection of EV chargers depended on the maximum charging power of every car that used the charger during the simulated week. For each charger, the maximum charging power seen during the week was examined prior to the simulations, if the maximum charging power during the week was 7.4 kW, the charger would be connected to a random single phase. If at any point during the week a vehicle with a charging power of 16 or 22 kW used the charger, the charger would be connected three-phase.

4.4 LCT Distribution

In this study, the increased penetration of LCTs is modelled. For these simulations LCTs have to be assigned to buildings in increasing penetration levels. In the reference setting no LCTs are assigned. In real life, the penetration of LCTs will not be homogeneously distributed. People living in higher income areas tend to adopt new technologies more easily since they have more budget to spend, leading to a skewed distribution. The grids used in this study are too small to emulate income effects on the distribution of LCTs. Therefore in this study the LCTs are randomly distributed in the electricity grid.

Another simplification of real life is used in the simulation of the increase of penetration. In reality, households using PVs, EVs and heat pumps will most likely continue to do so in the future. This is not accounted for in the simulations, for each increase, all LCTs are reassigned to random locations.

A third simplifications is that no ties are assumed between different LCTs. In reality, for example, a household with a PV system is more likely to also have an EV and/or a heat pump.

4.5 Experiments

Several experiments were performed: first a reference simulation was performed for each of the six grids without added LCTs to investigate existing unbalance in the different grids.

Then, simulations of increasing levels of LCT penetration (50%, 80%, 100%) were performed, where 50% emulates the near future, 80% the far future and 100% the year 2050 [36]. In these simulations LCTs were positioned in varying combinations (PV & EV, PV & HP and PV & EV & HP) at their original locations as used in [36], to compare to former, balanced simulation results [36]. The maximum and mean VUF was determined.

To show the impact of the locations of the LCTs, the LCTs were connected to random nodes in the network. Home LCTs, PV systems, heat pumps and private EV chargers, were restricted to home nodes. Public and semi-public EV chargers were distributed over the remaining nodes. No LCT of the same type could be connected to the same node. This process was performed 10 times for each LCT penetration level, excluding 0% penetration, as there are no LCTs in that scenario. The amount of iterations was decided to be 10 to strike a balance between the computing time and a representative sample size. The random number generators used to generate the phase connections for single-phase LCTs were reseeded after every iteration to exclude the influence of different phase connections.

This process was performed both for a winter scenario as well as a summer scenario to show the impact of different seasons on three-phase unbalance.

Finally, the power consumed by EV chargers and heat pumps was reduced, to investigate the impact of a simple EV charging control scheme as well as a simple energy consumption reduction of the heat pumps. Again, simulations were performed for different LCT locations and LCT penetration levels (0%, 50%, 100%) for a winter week.

5 Initial Load Locations

5.1 Results

Figure 5.1 shows the voltage unbalance in the different grids for increasing LCT penetration levels, where the LCTs are connected to the original load locations as in [36]. It can be seen that the lightly loaded rural grid (top left) maintains low voltage unbalance for all levels of LCT penetration. Even for 100% penetration, the maximum VUF stays below 0.35%. For four of the five other grids (light suburban & urban grids and heavy rural & urban grids), the maximum unbalance is below 3.5%. Only the heavy suburban grid (bottom middle) exceeds 3.5% for 80% and 100% LCT penetration, reaching a maximum VUF of 7.5%. It is clear that the VUF is not strictly linearly related to the LCT penetration levels. For some grids (light suburban & urban and heavy rural) the unbalance decreases with increasing LCT penetration.

Comparing the different LCTs used, it can be seen that the unbalance is higher for heat pumps than for EV chargers for almost all grids and LCT penetration levels. The only exception is seen in the heavy rural grid for 80% LCT penetration. For both the light rural (top left) and heavy urban grid (bottom right), it can be seen that the unbalance in the scenario PV+EV+HP is very close to the unbalance in the scenario PV+HP. The addition of EV chargers to the grids has very little impact on the unbalance for these two grids.

The heavily loaded rural grid (bottom left) has higher voltage unbalance than the light rural grid, as it is more heavily loaded. At 100% penetration, the VUF is approximately 3.5 times as high. The same effect can be seen for the suburban grids, however, the heavily loaded suburban grid (bottom middle) exceeds the legal limit of 3% [22] for high penetration levels of PV systems EV chargers and heat pumps combined. Even for only PV and heat pumps combined, the limit of 3% is reached for 80 and 100% penetration. Unexpectedly, the heavily loaded urban grid (bottom right) has lower voltage unbalance than its lightly loaded counterpart.

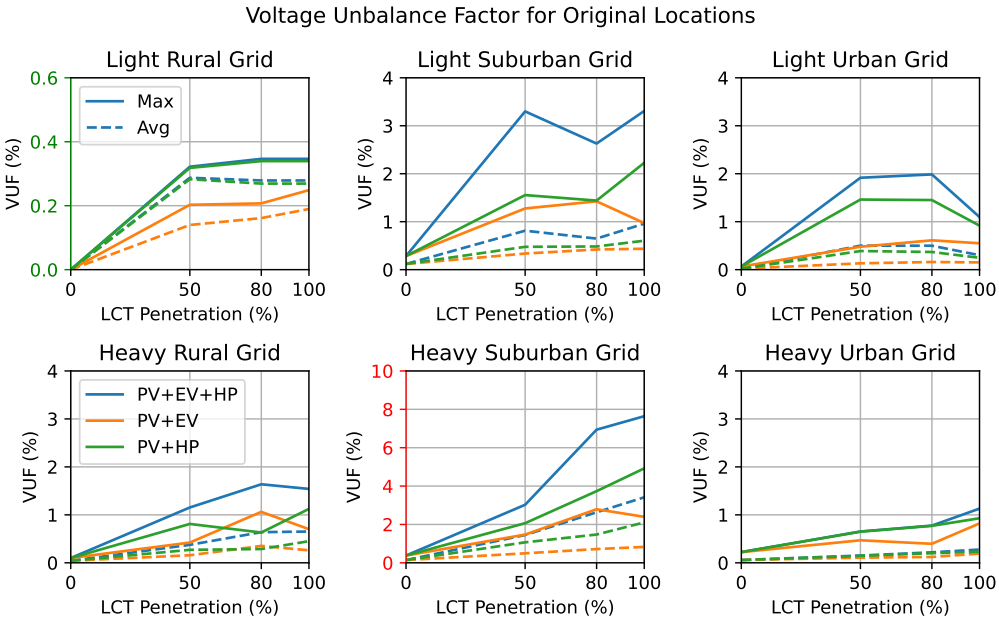

Figure 5.1: Maximum and average voltage unbalance factor using the original load locations for increasing LCT penetration levels for different combinations of LCTs. The top row shows the lightly loaded grids, the bottom row shows the heavily loaded grids.

As the Autoriteit Consument & Markt (ACM) obligates DSOs to maintain a VUF lower than 3% for 95% of the time at the point of common coupling [41], the duration of unbalance exceeding certain levels was investigated.

The duration that the average building experiences various levels of voltage unbalance during one week is shown in Figure 5.2. Once again it is clear that the heavy suburban grid has the highest peak unbalance, being the only grid exceeding 3% for any amount of time. Buildings in the heavily loaded rural grid experience a voltage unbalance factor of 0.5% longer than 6 hours a week on average.

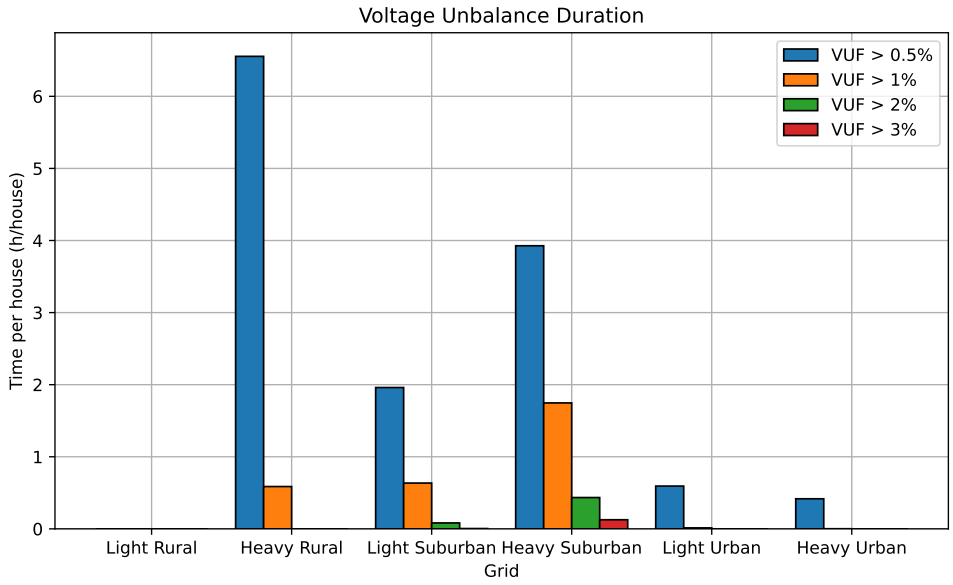

Figure 5.2: Hours per week of maximum VUF exceeding various values for 100% PV, EV and heat pump penetration

5.2 Grid Comparison

For the rural and suburban grids it is clear that the heavily loaded grids suffer higher voltage unbalance than the lightly loaded grids. However, this is not the case for the urban grids, as the voltage unbalance is higher in the lightly loaded urban grid than it is in the heavily loaded urban grid.

5.2.1 Rural Grids

The voltage unbalance in the heavily loaded rural grid exceeded the voltage unbalance in the lightly loaded rural grid in all scenarios. This is due to the fact the heavily loaded grid contains far more loads than the lightly loaded grid, as shown in Table 4.1. This means that the heavily loaded rural grid will contain far more LCTs, the majority of which are single-phase, causing 3-phase unbalance.

5.2.2 Suburban Grids

The suburban grids show the same pattern, the heavily loaded grids suffer more 3-phase unbalance in all scenarios. Again, this can partially be explained by the fact that the heavily loaded suburban grid contains more loads than the lightly loaded suburban grid as shown in Table 4.1. Another factor contributing to the high unbalance in thee heavily loaded suburban grid is that energy is consumed at longer distances from the external grid as shown in Figure 5.3.

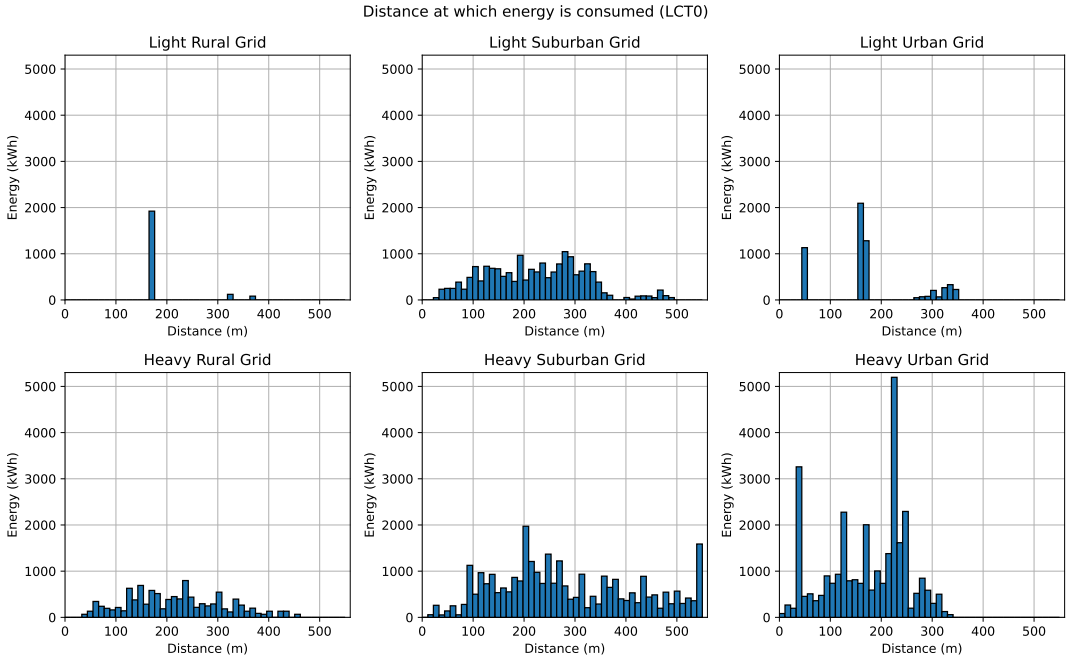

Figure 5.3: Histogram of the distance from the LV side of the transformer at which the base load energy is consumed for each grid.

5.2.3 Urban Grids

The urban grids do not follow the same pattern as the rural and suburban grids, as 3-phase unbalance is similar in the lightly loaded and heavily loaded urban grid when LCTs are added to the grids. In the scenario of the original LCT locations, unbalance in the lightly loaded grid exceeds that of the heavily loaded grid. In the base case, without added LCTs, the heavily loaded grid suffers higher unbalance than the lightly loaded grid.

Figure 5.4 visualizes the distance at which energy is consumed in the open-ended feeders in the grids, normalized to the the length of each feeder. It can be seen that energy consumption in the lightly loaded urban grid occurs almost exclusively at the farthest point of the feeders (two feeders are empty), while energy consumption in the heavily loaded urban grid occurs at around three quarters into the feeder. This could explain thee more sever unbalance issues in the lightly loaded urban grid compared to the heavily loaded urban grid.

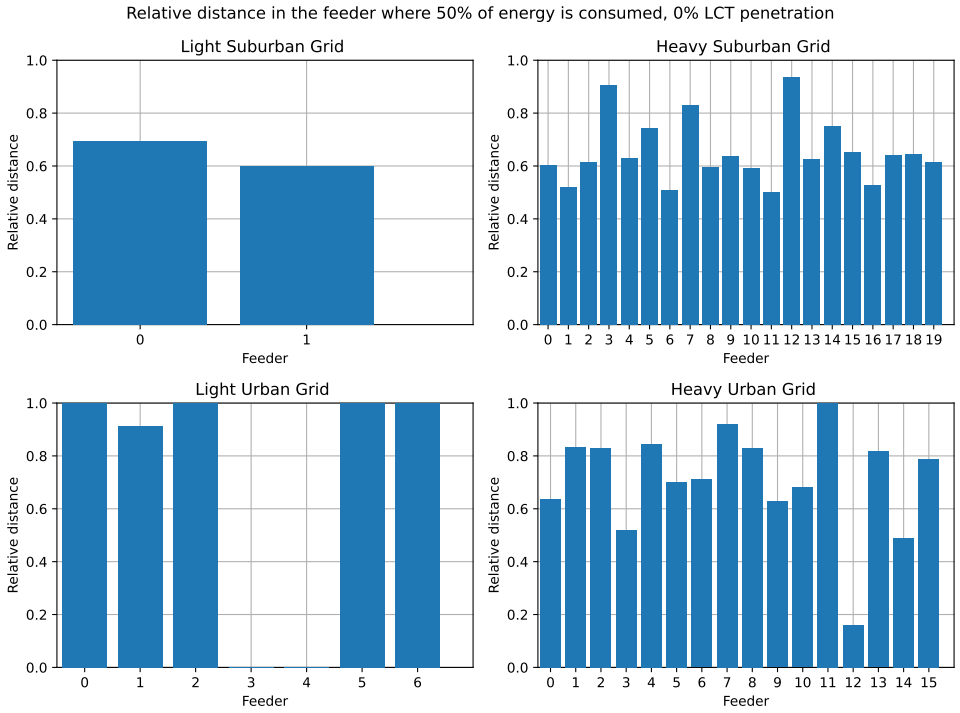

Figure 5.4: Visualization of the distance in the feeders at which energy is consumed.

Table 5.1 shows the percentage of loads that are connected to open-ended feeders. The rural and urban grids consist only of open-ended feeders, while the suburban grids service loads through a combination of meshed and open-ended feeders as can also be seen in Figures 4.1, 4.2 and 4.3. This means that the determination of the distance of energy consumption in open-ended feeders is not as applicable to the suburban grids as it is to the urban grids.

Grid	% **Loads in feeders**
Light Rural	100%
Heavy Rural	97.8%
Light Suburban	19.5%
Heavy Suburban	78.3%
Light Urban	100%
Heavy Urban	99.7%

Table 5.1: The share of base load in open ended feeders

5.2.4 LCT Comparison

Three combinations of LCTs were used to investigate their unbalance impact. The results show that as expected, the largest 3-phase unbalance occurs when the three LCTs, PV systems, heat pumps and EV chargers were used. It is also clear that heat pumps have a higher

unbalance impact than EV chargers as the PV & heat pump scenario consistently has higher unbalance than the PV & EV charger scenario.

Part of the reason heat pumps have a higher unbalance impact is that every heat pump is a single-phase component, where only 16.2% of EV chargers are single-phase. Another contributing factor is that relative to EV chargers, heat pumps consume more energy and are active for more time during the day.

6 LCT Locations

6.1 Results

The maximum voltage unbalance varies with the locations of the LCTs as can be seen in Figure 6.1. Similar to the results for the initial load locations, the light rural grid maintains the lowest voltage unbalance while the heavy suburban grid experiences the highest voltage unbalance. Irrespective of the LCTs used, the median maximum VUF increases for increasing LCT penetration.

The unbalance in the scenario PV+EV+HP is similar to the unbalance in the scenario PV+HP. In most grids, the addition of EV chargers to the grids has a smaller impact on the unbalance than the addition of heat pumps. However, for the heavy rural grid and the light suburban grid, the median VUF is higher for the PV+EV scenario than for the PV+HP scenario.

As expected, there is no variation for the 0% LCT penetration scenario as there are no LCTs to be connected to different locations. The voltage unbalance in this case is only due to unbalanced base load. Variance in the unbalance levels is similar in every grid, with the range increasing as the median unbalance increases. Like in Figure 5.1, the lightly loaded urban grid and heavily loaded urban grid suffer similar levels of voltage unbalance.

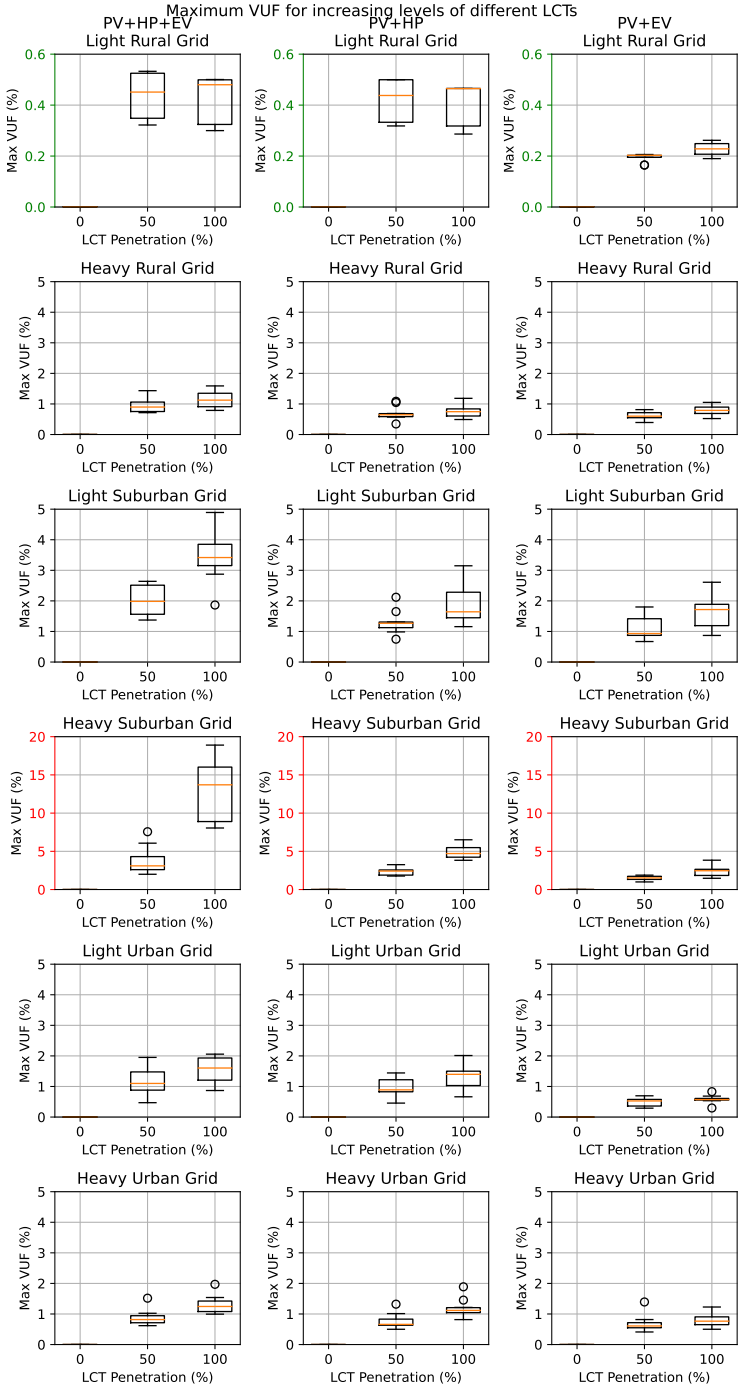

Figure 6.1: Boxplot of the maximum VUF for 10 iterations of randomized LCT locations for increasing LCT penetration levels. Three scenarios of different LCTs were used from left to right: PV+HP+EV, PV+HP and PV+EV.

In Figure 6.2, the median VUF of the different scenarios (PV+HP and PV+EV) is plotted against the median VUF of the scenario PV+HP+EV. If the influence of the EV chargers is negligible, the markers of the PV+HP scenario would lie on the identity line (dashed grey). This means that the vertical distance to the identity line can be interpreted as the impact of the omitted LCT. For four of the six grids, the markers are nearly on the identity line, indicating that the unbalance impact of EV chargers is limited. In the light and heavy suburban grids, the addition of EV chargers does have an impact on the voltage unbalance.

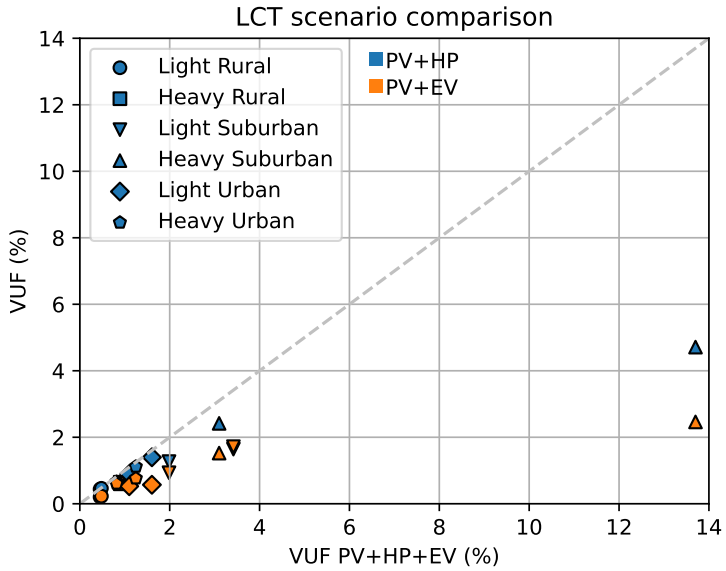

Figure 6.2: The median VUF of the different scenarios (PV+HP and PV+EV) plotted versus the median VUF of the scenario PV+HP+EV.

Figure 6.3 shows how long the VUF exceeded various thresholds for each grid on average. The error-bars represent the maximum and minimum durations obtained in the 10 iterations. It can be seen that on average, every building in the heavy suburban grid experiences 0.1 hours (6 min.) of voltage unbalance larger than 3% VUF. Once again, the lightly loaded urban grid is more impacted than the heavily loaded urban grid, experiencing voltage unbalance for longer than the heavily loaded urban grid.

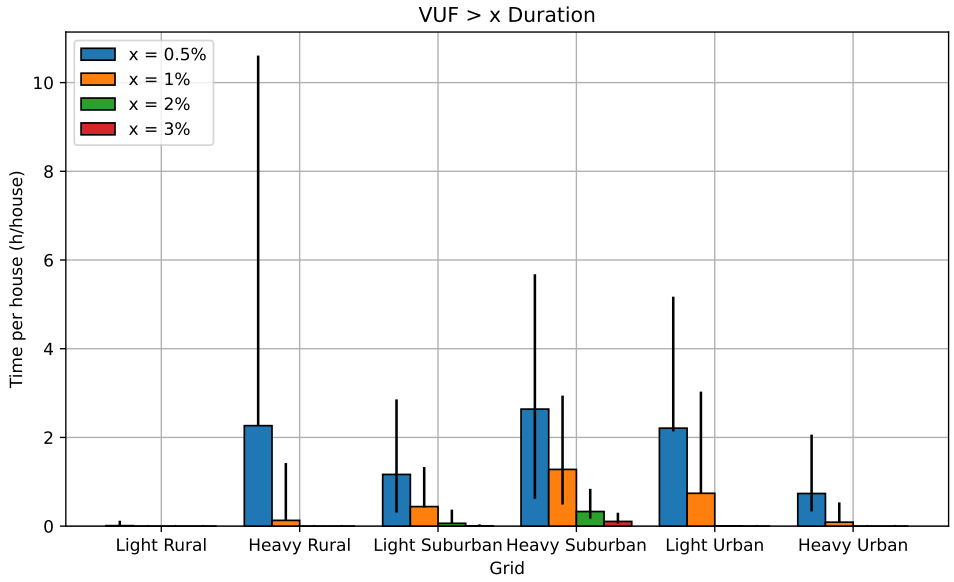

Figure 6.3: Duration of maximum VUF exceeding various values for 100% LCT penetration

7 Seasons

7.1 Results

Figure 7.1 shows the maximum and average voltage unbalance during a summer week, for the different grids and LCT scenarios. For four of the grids, the unbalance values are slightly lower than for the winter week in the scenario with all LCTs. Where the unbalance impact of heat pumps is decreased in the summer week relative to the winter week, the unbalance impact of EV chargers is increased in the summer week. In the suburban grids and the heavy rural grid, EV chargers have a higher voltage unbalance impact than heat pumps.

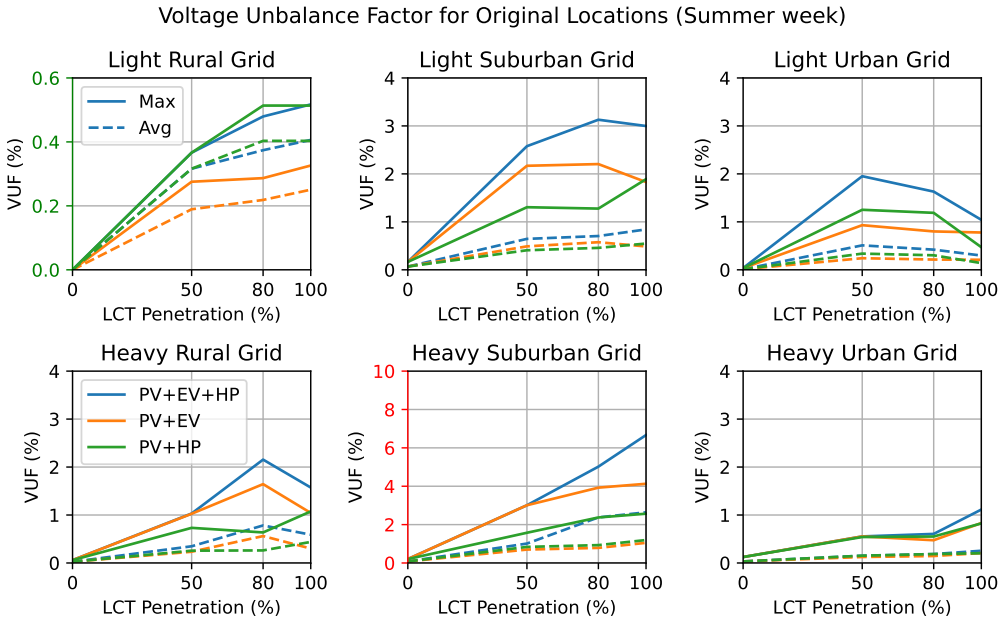

Figure 7.1: Maximum and average voltage unbalance factor using the original load locations for increasing LCT penetration levels for different combinations of LCTs in the summer. The top row shows the lightly loaded grids, the bottom row shows the heavily loaded grids.

The duration of various unbalance levels during a summer week for 100% LCT penetration is shown in Figure 7.2. The results are similar to those of the winter week, albeit lower in magnitude, apart from the light rural grid, which exceeds 0.5% for 7 minutes in the week on average. The duration that the VUF exceeds 0.5% in the heavy rural grid is halved for the summer week relative to the winter week.

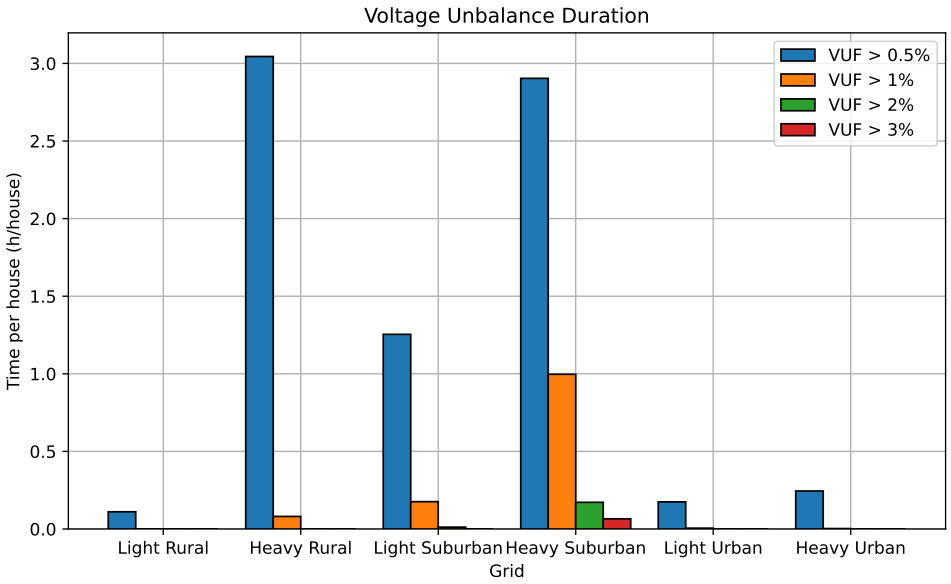

Figure 7.2: Hours per summer week of maximum VUF exceeding various values for 100% PV, EV and heat pump penetration

7.2 Discussion

The season in which the simulation takes place affects the base load and LCTs in different ways. In the summer week, PV generation is increased relative to the winter week as the solar irradiance is increased. EV charger energy consumption is reduced relative to the winter week, as less energy is spent heating the vehicles. Similarly, heat pump and base load power consumption in the summer week is reduced relative to the winter week.

In all grids, the different scenarios show different responses to the change in season. Unbalance for the scenario with all LCTs remains more or less the same, while the PV+heat pump (HP) scenario shows a decrease in unbalance in the summer. The PV+EV scenario on the other hand, shows an increase in unbalance in the summer. The results for the scenario with all LCTs are as expected as the increase in PV power generation and the decrease in EV charger and heat pump power consumption counteract eachother, and the base load has little impact on unbalance in general. Voltage unbalance in the scenario using only PV systems and heat pumps is expected to decrease due to the decrease in heat pump power, which is reflected in the results. Unbalance levels for the scenario containing only PV systems and EV chargers increase. This is likely due to the fact that the unbalance impact of the increase in PV generation exceeds that of the decrease in EV charger energy consumption. Furthermore,

as PV generation and EV charger consumption happen mainly during the daytime, the share of solar energy consumed by the EV chargers is reduced in the summer, further increasing unbalance.

8 Control

8.1 Results

The results of simulations of selected grids using a simple LCT control scheme are shown next to the original results in Figure 8.1. It can be seen that the LCT control scheme causes an increase in maximum voltage unbalance in the suburban grid in the PV+EV+HP and PV+EV scenarios. In all three grids, the LCT control scheme reduces the maximum unbalance in the PV+HP scenario. In the urban grids, the LCT control scheme is successful in reducing unbalance for the PV+EV+HP scenario. However, for the PV+EV scenario, this is not the case. An increase in unbalance is shown when the control scheme is introduced.

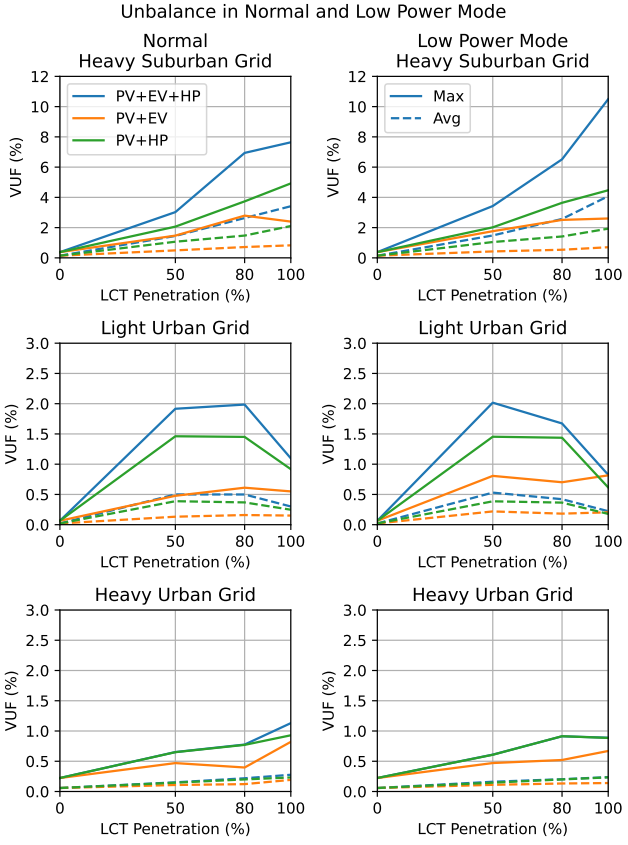

Figure 8.1

Figure 8.2 shows the duration of unbalance in the grids, compared to the original results. It can be seen that the duration the unbalance exceeds various limits is decreased for all grids when using the LCT control scheme.

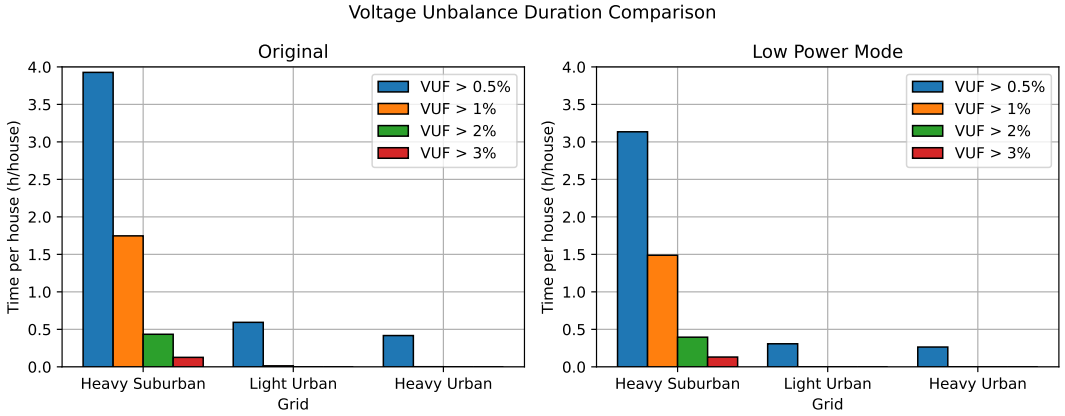

Figure 8.2: Comparison of the unbalance duration, 100% LCT penetration at original locations

8.2 Discussion

The simple EV charger and heat pump control schemes that were implemented had varying effects on the unbalance metrics. The control schemes were not always effective in reducing the maximum and average VUF that were measured during the week. This was to be expected, as the reduction in heat pump power consumption was very limited as the target temperature range was reduced from [21°C, 23°C] to [20°C, 21°C]. For the EV chargers, energy consumption remained the same as in the uncontrolled case, however, peak power consumption was reduced.

9 Conclusion

In view of the increasing electrification of the residential sector, where many LCTs will be connected to a single phase of a three-phase network, insight in the effect on three-phase unbalance is vital. Simulations were performed on six different grids, varying in level of urbanization and loading, with increasing levels of LCT penetration (0%, 50%, 80%, 100%). In these simulations, LCTs were integrated in varying combinations (PV & EV, PV & HP and PV & EV & HP). The maximum and mean VUF was determined. The effect of season and an LCT control scheme was evaluated.

Simulations showed that voltage unbalance exceeded the legal limit of 3% for two of the six grids for high levels of LCT penetration when all LCTs are integrated. Combining all three LCTs resulted in the highest unbalance levels. Varying the locations of the LCTs resulted in significant variations in unbalance levels. Comparing a winter week with a summer week, the overall unbalance is similar, however, the contribution of the PV systems to the unbalance is increased, while the contribution of EV chargers and heat pumps is decreased. The effect of the LCT control scheme was limited.

9.1 Impact of Grids

It can be concluded that the level of three-phase unbalance in the grid is affected by the distributional area. The grid with the least buildings, the light rural grid, is the least affected of the grids considered. The grid containing the most buildings, the heavy suburban grid, is the most heavily affected grid. Topology of the grid was also shown to be an important factor in determining the three-phase unbalance impact, as the grid with predominantly end-loaded feeders suffered worse unbalance than a more heavily loaded grid from the same distributional area whose feeders were not as end-loaded.

9.2 Impact of different LCTs

In general, it can be concluded that the combination of PV systems, EV chargers and heat pumps introduce more three-phase unbalance in the grids than the LCTs do separately. Furthermore, heat pumps consistently have a higher unbalance impact than EV chargers. This is likely due to the fact that all heat pumps are single-phase connected, where EV chargers are three-phase connected a large amount of the time.

9.3 Impact of Locations

The locations of the added LCTs have a significant impact on the level of three-phase unbalance. Even in the 2050 scenario where LCT penetration has reached 100%, where the LCTs are merely shuffled, the variance in three-phase unbalance is significant.

9.4 Impact of Seasons

Seasonal effects did not have a significant impact on overall three-phase unbalance, however, the individual impacts of the different LCTs were significantly affected. This should be taken into account when designing LCT control schemes.

9.5 Impact of LCT control

Since the chosen control scheme was not effective in reducing the voltage unbalance in the simulations, more impactful control schemes should be designed. These should take into account the state of the distribution network, in order to optimize the grid performance.

9.6 Limitations

Several limitations of the models and simulations have been identified.

The simulation uses only one model of each LCT. While randomization has been introduced in the power consumption and generation profiles of these LCTs, it is unrealistic to assume that each consumer will use the same component for each LCT.

In the simulations, it was assumed that the LCTs were homogeneously distributed over the buildings in the grid. However, this is not an accurate representation of reality, as early adopters of LCTs will primarily be high income households. High income households are often not distributed homogeneously over a region, they are usually concentrated in certain neighbourhoods. This effect is not taken into account in this thesis, as the grids are too small to be able to realistically emulate the effect.

9.7 Future Work

In future work, various more impactful LCT control schemes could be implemented to investigate the limits of LCT control.

Bibliography

[1] C. Fetting, "The european green deal," *ESDN Report*, December 2020.

[2] P. Bojek, "Solar pv," IEA, Paris, Tech. Rep., 2022.

[3] L. Cozzi, "The future of heat pumps," IEA, Tech. Rep., 2022.

[4] O. Alsauskas, E. Connelly, A. Daou, A. Gouy, M. Huismans, H. Kim, J. Le Marois, S. McDonagh, A. Petropoulos, and J. Teter, "Global ev outlook 2023," IEA, Tech. Rep., 2023.

[5] H. De Jonge, "Normering hybride warmtepompen," May 2022. [Online]. Available: https://open.overheid.nl/documenten/ronl-1b13f0fa73aeda00fffa1c07c120222dd00932af/pdf

[6] "Regulation (eu) 2023/851 of the european parliament and of the council," p. 5, May 2023.

[7] 2023. [Online]. Available: https://capaciteitskaart.netbeheernederland.nl/

[8] K. Ma, L. Fang, and W. Kong, "Review of distribution network phase unbalance: Scale, causes, consequences, solutions, and future research directions," *CSEE Journal of Power and Energy Systems*, vol. 6, no. 3, pp. 479–488, 2020.

[9] *Voltage Characteristics of Electricity Supplied by Public Electricity Networks*. NEN-EN 50160, 2022.

[10] J. Conzade, F. Nägele, S. Ramanathan, and P. Schaufuss, "Europe's ev opportunity—and the charging infrastructure needed to meet it," McKinsey, Tech. Rep., 2022.

[11] E. Clarke, "Simultaneous faults on three-phase systems," *Transactions of the American Institute of Electrical Engineers*, vol. 50, no. 3, pp. 919–939, 1931.

[12] K. Ma, R. Li, and F. Li, "Quantification of additional asset reinforcement cost from 3-phase imbalance," *IEEE Transactions on Power Systems*, vol. 31, no. 4, pp. 2885–2891, 2016.

[13] "Ieee standard test procedure for polyphase induction motors and generators," *IEEE Std 112-1991*, pp. 1–, 1991.

[14] A. K. Singh, G. K. Singh, and R. Mitra, "Some observations on definitions of voltage unbalance," in *2007 39th North American Power Symposium*, 2007, pp. 473–479.

[15] P. Pillay and M. Manyahe, "Definitions of voltage unbalance," *IEEE Power Engineering Review*, vol. 21, no. 5, pp. 49–51, 2001.

[16] C. J. Fechheimer, "Power factor and unbalance on a polyphase system," *Journal of the American Institute of Electrical Engineers*, vol. 39, no. 6, pp. 545–546, 1920.

[17] G. Chicco, F. Corona, R. Porumb, and F. Spertino, "Experimental indicators of current unbalance in building-integrated photovoltaic systems," *IEEE Journal of Photovoltaics*, vol. 4, no. 3, pp. 924–934, 2014.

[18] Y.-J. Wang, "Analysis of effects of three-phase voltage unbalance on induction motors with emphasis on the angle of the complex voltage unbalance factor," *IEEE Transactions on Energy Conversion*, vol. 16, no. 3, pp. 270–275, 2001.

[19] D. Sharon, J.-C. Montano, A. Lopez, M. Castilla, D. Borras, and J. Gutierrez, "Power quality factor for networks supplying unbalanced nonlinear loads," *IEEE Transactions on Instrumentation and Measurement*, vol. 57, no. 6, pp. 1268–1274, 2008.

[20] "Ieee recommended practice for electric power distribution for industrial plants," *IEEE Std 141-1993*, pp. 1–768, 1994.

[21] A. I. Adekitan, "A new definition of voltage unbalance using supply phase shift," *Journal of Control, Automation and Electrical Systems*, vol. 31, no. 3, pp. 718–725, 2020.

[22] Nederland, "Artikel 7.3c," *Netcode Elektriciteit*. [Online]. Available: https://wetten.overheid.nl/jci1.3:c:BWBR0037940&hoofdstuk=7&paragraaf=7.2&artikel=7.3&z=2023-05-11&g=2023-05-11

[23] F. Shahnia, R. Majumder, A. Ghosh, G. Ledwich, and F. Zare, "Voltage imbalance analysis in residential low voltage distribution networks with rooftop pvs," *Electric Power Systems Research*, vol. 81, no. 9, pp. 1805–1814, 2011. [Online]. Available: https://www.sciencedirect.com/science/article/pii/S0378779611001040

[24] F. Ruiz-Rodriguez, J. Hernández, and F. Jurado, "Voltage unbalance assessment in secondary radial distribution networks with single-phase photovoltaic systems," *International Journal of Electrical Power & Energy Systems*, vol. 64, pp. 646–654, 2015. [Online]. Available: https://www.sciencedirect.com/science/article/pii/S0142061514005158

[25] C. Gonzalez, J. Geuns, S. Weckx, T. Wijnhoven, P. Vingerhoets, T. De Rybel, and J. Driesen, "Lv distribution network feeders in belgium and power quality issues due to increasing pv penetration levels," in *2012 3rd IEEE PES Innovative Smart Grid Technologies Europe (ISGT Europe)*, 2012, pp. 1–8.

[26] O. Mrehel and A. A. Issa, "Voltage imbalance investigation in residential lv distribution networks with rooftop pv system," in *2022 IEEE 2nd International Maghreb Meeting of the Conference on Sciences and Techniques of Automatic Control and Computer Engineering (MI-STA)*, 2022, pp. 655–662.

[27] J. Aramizu and J. C. M. Vieira, "Analysis of pv generation impacts on voltage imbalance and on voltage regulation in distribution networks," in *2013 IEEE Power And Energy Society General Meeting*, 2013, pp. 1–5.

[28] J. M. Sexauer and S. Mohagheghi, "Voltage quality assessment in a distribution system with distributed generation—a probabilistic load flow approach," *IEEE Transactions on Power Delivery*, vol. 28, no. 3, pp. 1652–1662, 2013.

[29] G. A. Putrus, P. Suwanapingkarl, D. Johnston, E. C. Bentley, and M. Narayana, "Impact of electric vehicles on power distribution networks," in *2009 IEEE Vehicle Power and Propulsion Conference*, 2009, pp. 827–831.

[30] A. Ul-Haq, C. Cecati, K. Strunz, and E. Abbasi, "Impact of electric vehicle charging on voltage unbalance in an urban distribution network," *Intell Ind Syst*, vol. 1, pp. 51–60, 2015.

[31] L. Mejdi, F. Kardous, and K. Grayaa, "Impact analysis and optimization of ev charging loads on the lv grid: A case study of workplace parking in tunisia," *Energies*, vol. 15, no. 19, 2022. [Online]. Available: https://www.mdpi.com/1996-1073/15/19/7127

[32] M. J. M. Al Essa and L. M. Cipcigan, "Integration of renewable resources into low voltage grids stochastically," in *2016 IEEE International Energy Conference (ENERGYCON)*, 2016, pp. 1–5.

[33] Y. Li and P. A. Crossley, "Monte carlo study on impact of electric vehicles and heat pumps on lv feeder voltages," in *12th IET International Conference on Developments in Power System Protection (DPSP 2014)*, 2014, pp. 1–6.

[34] Enexis, 's-Hertogenbosch, Nederland. [Online]. Available: https://www.enexis.nl/

[35] NEDU, "Profielen elektriciteit 2018," 2018. [Online]. Available: https://web.archive.org/web/20181202215314/https://www.nedu.nl/documenten/verbruiksprofielen/

[36] N. Damianakis, "Coordinated power control in future sustainable dc power grid," Ph.D. dissertation, Delft University of Technology, Delft, 2022.

[37] Meteonorm. [Online]. Available: https://meteonorm.com/en/

[38] A. H. Smets, K. Jäger, O. Isabella, R. van Swaaij, and M. Zeman, *Solar Energy: The physics and engineering of photovoltaic conversion technologies and systems*. UIT, 2016.

[39] ev database, Amsterdam, Nederland. [Online]. Available: https://ev-database.org/

[40] N. Damianakis, G. R. Chandra Mouli, and P. Bauer, "Risk-averse estimation of electric heat pump power consumption," in *2023 IEEE Transportation Electrification Conference & Expo (ITEC), Accepted*, 2023.

[41] Nederland, "Artikel 2.33," *Netcode Elektriciteit*. [Online]. Available: https://wetten.overheid.nl/jci1.3:c:BWBR0037940&hoofdstuk=2&paragraaf=2.4&artikel=2.33&z=2023-05-11&g=2023-05-11

Colophon

This document was typeset using LaTeX, using the KOMA-Script class `scrbook`. The main font is Palatino.